Supplementary Information

Supramolecular Core-Shell Heterostructures with Controllable Multi-Color-Emitting Properties

Hongyang Zhang,[a,b] Yilong Lei,[a,b] Haitao Wang,[b] and Wai-Yeung Wong*[a,b]

Dr. H. Zhang, Dr. Y. Lei, Prof. W.-Y. Wong
Department of Applied Biology and Chemical Technology, The Hong Kong Polytechnic University,
Hong Kong (China)
E-mail: wai-yeung.wong@polyu.edu.hk

Dr. H. Zhang, Dr. Y. Lei, H. Wang, Prof. W.-Y. Wong
Department of Chemistry, Institute of Molecular Functional Materials, Hong Kong Baptist University,
Hong Kong (China)

Table of Contents

Experimental Section

Materials. Dibenzothiophene, fluorene, carbazole and 1,2,4,5-tetracyanobenzene (TCNB) were purchased from Sigma-Aldrich and TCI, respectively, and used without further treatment. For the solvents, acetonitrile (A.R.) and ethanol (A.R.) were purchased from RCI Labscan Ltd., Thailand. Ultrapure water with a resistivity of 18.2 MΩ•cm at 25 °C was produced by using a Milli-Q apparatus of Milipore Corporation.

Syntheses of single-crystalline CT microrods composed of the carbazole-type molecules and TCNB. The 1D singe-crystalline CT microrods composed of carbazole-type molecules and TCNB were prepared via a CT-induced self-assembly with the assistance of solvent etching. In a typical synthesis, 10 mL of a stock solution of dibenzothiophene (20 mM) was mixed rapidly with an equal volume of TCNB solution (20 mM) in acetonitrile under vigorous stirring. After several minutes, the resultant solution (2 mL) was injected into 5 mL of a 3:7 (v/v) ethanol/water mixture. Light-color flocculent suspension appeared within several seconds. Single-crystalline microrods of fluorene-TCNB and carbazole-TCNB complexes were also synthesized following the similar experimental procedure, except that the molecular concentration of fluorene with 1 eq. TCNB and carbazole with 1 eq. TCNB was set to 50 mM and 70 mM, respectively. The resultant colloidal samples were collected on the surface of a quartz substrate. In the meantime, part of the flocculent colloid was separated by centrifugation at 3500 rpm and washed several times with ultrapure water, and finally dried under vacuum for further analysis.

Syntheses of single-layer organic CT core-shell structures: S-TCNB@N-TCNB and C-TCNB@N-TCNB. In a typical experiment for S-TCNB@N-TCNB heterostructure, 1 mL of a stock solution of carbazole-TCNB complex in acetonitrile (35 mM) was prepared. Then for the growth of carbazole-TCNB domains, 10 mL suspension of dibenzothiophene-TCNB microrods was injected into 0.5 mL of as-prepared solution of carbazole-TCNB complex (35 mM), and allowed to stand for 0.5 hour, afterwards a cyan and orange blended suspension was formed. The resultant colloidal samples were purified using the same procedure as that for dibenzothiophene-TCNB microrods. For C-TCNB@N-TCNB core-shell heterostructure, the similar procedure was performed, except 10 mL suspension of fluorene-TCNB microrods was injected as the seed.

Syntheses of two-layer organic core-shell CT structures: S-TCNB@N-TCNB@C-TCNB and C-TCNB@N-TCNB@S-TCNB. After the syntheses of single-layer organic core-shell structures, the resultant colloidal samples were separated by centrifugation at 3500 rpm and immersed in a new 3:1 (v/v) ethanol/water mixed solvent to serve as seeds, then for a typical experiment of two-layer core-shell structures S-TCNB@N-TCNB@C-TCNB, 10 mL suspension of S-TCNB@N-TCNB seeds was injected into 0.5 mL of as-prepared solution of fluorene-TCNB complex (25 mM), while for C-TCNB@N-TCNB@S-TCNB core-shell heterostructure, the procedure was that 10 mL suspension of C-TCNB@N-TCNB seeds was injected to into 0.5 mL of as-prepared solution of dibenzothiophene-TCNB complex (10 mM).

Syntheses of three-layer organic CT core-shell structures: S-TCNB@N-TCNB@C-TCNB@N-TCNB and C-TCNB@N-TCNB@S-TCNB@N-TCNB. The syntheses of three-layer organic core-shell structures were performed by following the repetitive operation as that for two-layer organic core-shell structures, the differences are that the as-prepared two-layer core-shell structures serve as seeds and the carbazole-TCNB complex in acetonitrile (35 mM) serves as the growing constituent again.

Characterization. The morphologies and sizes of as-prepared samples were examined by utilizing field-emission scanning electron microscopy (LEO 1530 Field Emission SEM) at acceleration voltages of 20 kV. Prior to measurement, the as-prepared samples were coated with a thin gold layer using an SPI Module Sputter Coater. TEM photographs were obtained by means of a Tecnai G2 20 S-TWIN Transmission Electron Microscope operated at 120 or 200 kV. The samples were prepared by depositing one drop of colloidal dispersion on a carbon-coated copper grid, and dried at room temperature under high vacuum. The structural characterizations of the as-synthesized microrods and core-shell structures were performed via PXRD on a Bruker AXS D8 Advance X-Ray Diffractometer, with Cu Kα (Running condition: 40 kV, 40 mA) for analyzing the composition and phase purity. The fluorescence microscopy photographs were taken by using a Leica DMRBE fluorescence microscopy with the aid of a spot-enhanced charged couple device (CCD, Diagnostic Instrument, Inc.) and the samples were prepared by dropping the dispersion (100 μL) onto a cleaned quartz slide. Laser confocal fluorescent microscopy (Leica, TCS-SP5) equipped with near ultraviolet laser (405 nm) was employed for photographing fluorescent images besides recording micro-area PL spectra of single-crystalline CT complex microrods and core-shell heterostructures. In addition, for the single-crystal analyses, X-ray diffraction data were collected at 173 or 100 K using graphite-monochromated Mo-Kα radiation (λ = 0.71073 Å) with a Bruker APEX II CCD diffractometer. The collected frames were processed with the software SAINT+ and an absorption correction (SADABS) was applied to the collected reflections. The structure was solved by direct methods (SHELXTL) in conjunction with standard difference Fourier techniques and subsequently refined by full-matrix least-squares analyses on F^2. Hydrogen atoms were generated in their idealized positions and all nonhydrogen atoms were refined anisotropically. CCDC-1893693, CCDC-1893695 and CCDC-1893697 contains the supplementary crystallographic data for this paper. These data can be obtained free of charge from The Cambridge Crystallographic Data Centre via www.ccdc.cam.ac.uk/ data_request/cif.

Other Supporting Information

For the more detailed characterization, we conducted the XRD tests of all the single-layer core-shell microrods and multi-layer core-shell microrods that we have fabricated. By comparing with all three pure TCNB-based CT complexes, we found they share almost the same pattern, in which two characteristic peaks between 10 to 15 degree are indexed to (110) and (020) lattice planes (Figure S1).[1] More SEM and TEM images about three pure TCNB-based CT complexes are shown in Figure S2, which show a rectangular cross-section with a diameter of several micrometers, and a length of tens of micrometers. Additionally, their fluorescent microscopy and LCFM images for individual microrod show more specific details in a high magnification (Figure S3). The SEM and TEM images of formed single-layer core-shell microrods or multi-layer core-shell microrods reveal that no obvious change of exterior shape happened when the second constituent grew on the performed seeds, but you can still find some special cases among the large amount of SEM observations that the second constituent didn’t grow so perfectly on the former constituent, with a little crack or flaw on the surface of formed heterojunction (Figure S4 a-c). Because the sizes of the prepared microrods are beyond the range of TEM measurement, it is hard to allow the electrons to transmit through the rods. Therefore, all the obtained TEM images are dark and cannot probe the inside architecture clearly (Figure S4 d-i). However, we tried the TEM energy-dispersive X-ray spectroscopy (EDS), and the results can well prove the core-shell structures (Figure S5). Figures S6 and S7 give more typical and distinct images about single-layer core-shell microrods S-TCNB@N-TCNB and two-layer core-shell microrods S-TCNB@N-TCNB@C-TCNB viewed from low to high magnification.

For confirmation of the formation of single-layer core-shell heterostructure C-TCNB@N-TCNB, fluorescence microscopy tests were performed to examine the configuration because different layers could be differentiated by their different emission colours. Figure S8b-e shows the corresponding images excited by UV and green light, respectively. As expected, an orange-emitting thin layer is deposited onto the surface of a green-emitting microrod upon excitation with UV light (Figure S8b, d). When the excitation light was converted into green light, the inner core almost becomes non-emissive, while the outer layer exhibits strong red light (Figure S8c, e). Thus, it is clearly confirmed that the N-TCNB layer was uniformly coated onto the surface of C-TCNB microrods, forming C-TCNB@N-TCNB core-shell structures. The corresponding micro-area PL spectrum of C-TCNB@N-TCNB core-shell structures at the core-shell junction shows two PL peaks at 540 nm at the short-wavelength range and a PL peak at 590 nm at the long-wavelength range. When compared to the PL peak of the core-shell structure at the tip (590 nm), it can be clearly confirmed that the two PL peaks at 540 nm should be derived from the inner C-TCNB core, while the PL peak at 590 nm should be originated from the outer N-TCNB layer (Figure S8f-k).

To confirm the formation of two-layer core-shell heterostructured microrods C-TCNB@N-TCNB@S-TCNB, from the fluorescence microscopy results shown in Figure S9b and d, we can see that the orange-emitting N-TCNB layer is coated by a thin yellow-emitting layer when excited by UV light that should be the layer S-TCNB due to the tiny doping of carbazole into the S-TCNB composition, which is similar to our previous case.[2] Upon excitation with green light, two junctions with the clear interface at the tip part were observed, indicating the formation of two-layer core-shell structure as well (Figure S9c, e). LCFM results further confirm that a tip of two-layer core-shell heterostructured microrod involves two junctions at the core-shell interfaces. The corresponding micro-area PL spectrum shows the PL band of the position in Figure S9i at 550 nm corresponds to S-TCNB with tiny doping of carbazole. The position in Figure S9h has a PL band at 575 nm that corresponds to S-TCNB overlapping with N-CTNB. Obviously, the PL bands of the positions in Figure S9f and g have quite similar spectral profiles, indicating that both of them were composed of all three constituent CT materials (Figure S9f-m). The above results clearly confirm the formation of two-layer C-TCNB@N-TCNB@S-TCNB core-shell structure.

For the single crystals of three TCNB-based CT complex precursors, we successfully grew and analyzed them. The crystal unit cell parameters of three CT complexes S-TCNB, C-TCNB and N-TCNB have almost identical lattice sizes and angles (Figure S10 and Table S1), which are coherent with the reported data as well.[3] Such uniform and indistinguishable crystallographic parameters make them rational and reasonable for one to continuously grow on another one. Therefore, the crystal data support our inference for the solution epitaxial growth mechanism of our synthetic core-shell heterostructures.

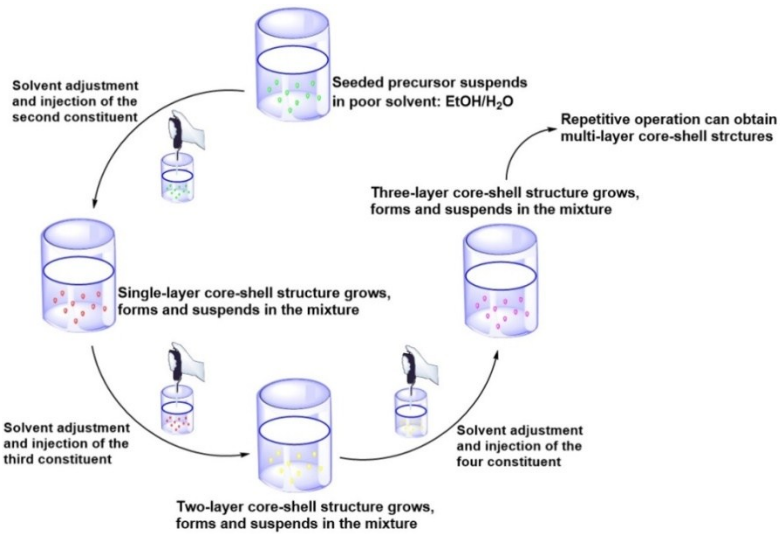

Chart S1. Prepared procedure and schematic illustration of using the stepwise seed-induced solution epitaxy method to form multi-layer core-shell heterostructured microrods.

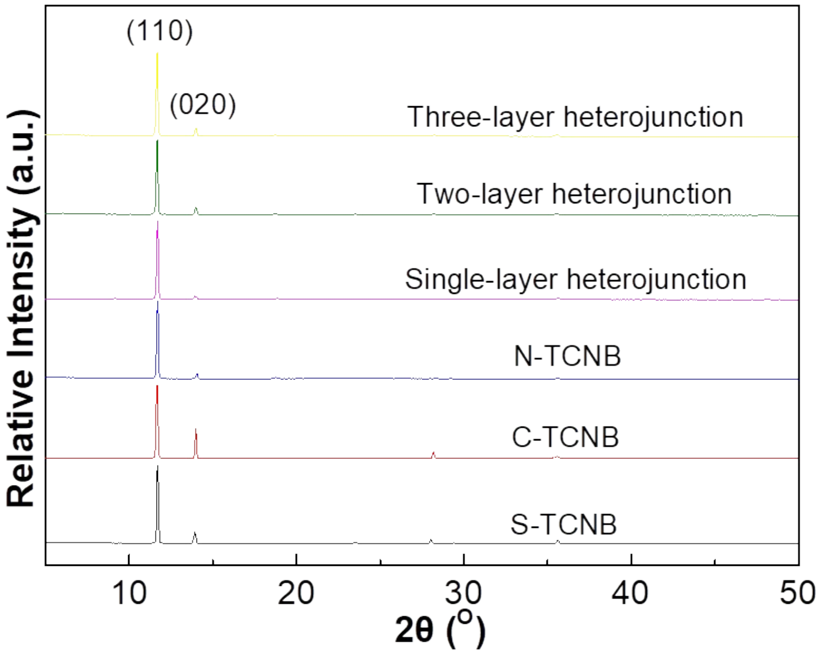

Figure S1. XRD patterns for S-TCNB microrods (black), C-TCNB microrods (red), N-TCNB microrods (blue), single-layer heterojunction (magenta), two-layer heterojunction (green) and three-layer heterojunction (yellow) deposited on the surface of a glass substrate.

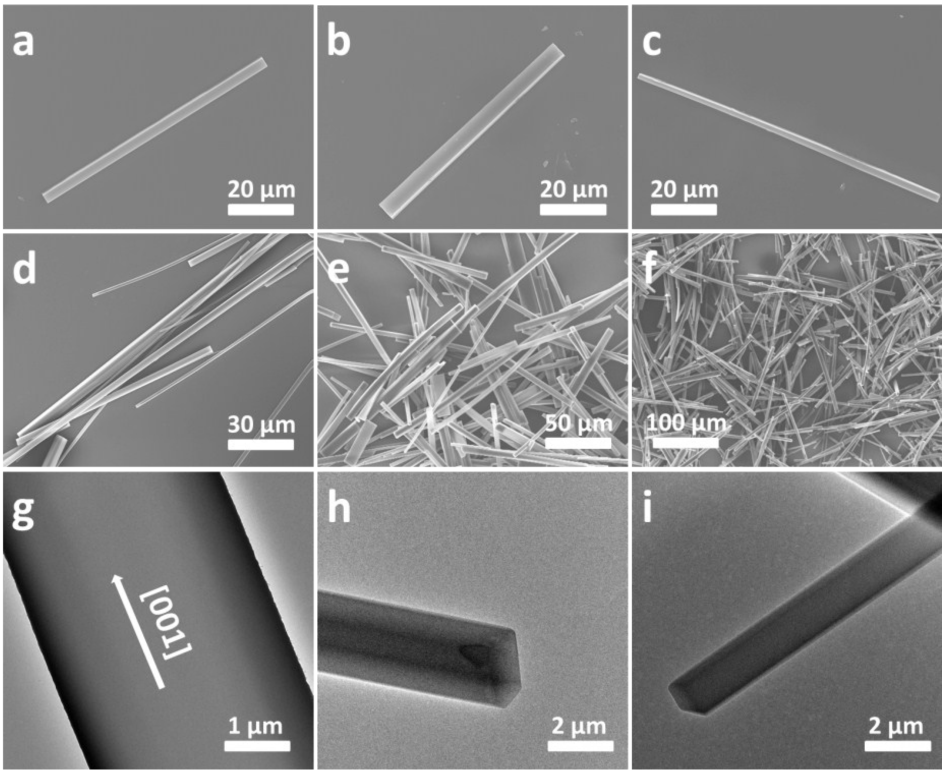

Figure S2. SEM images for individual S-TCNB microrods (a), individual C-TCNB microrods (b), individual N-TCNB microrods (c), carbazole-type molecules-TCNB mircrods viewed from high to low magnification (d-f), TEM images for individual carbazole-type molecules-TCNB mircrods at the body, tip and entirety (g-i).

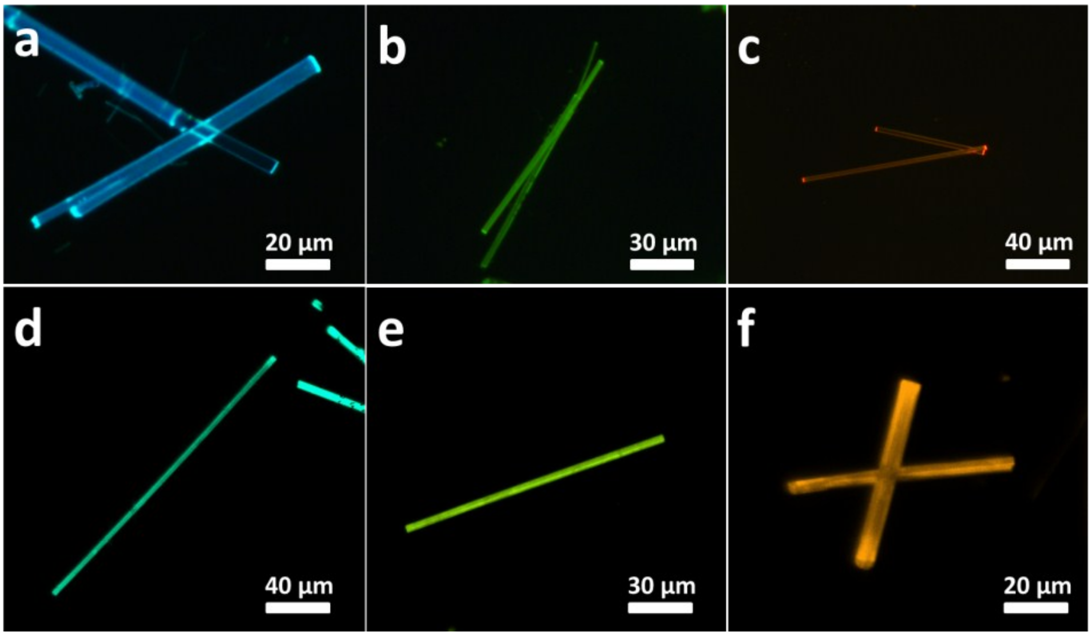

Figure S3. Fluorescent microscopy images for individual S-TCNB microrods (a), individual C-TCNB microrods (b), individual N-TCNB microrods (c), LCFM images for individual S-TCNB microrods (d), individual C-TCNB microrods (e), individual N-TCNB microrods (f).

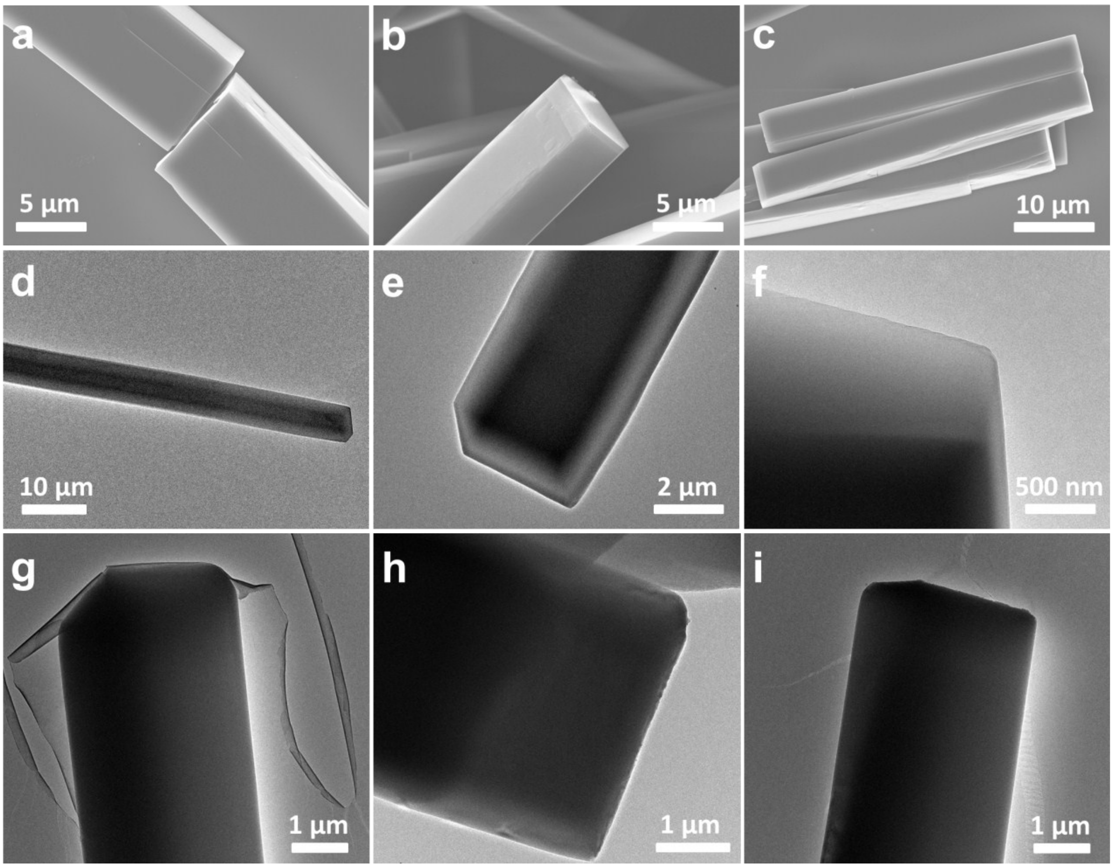

Figure S4. SEM images for the core-shell heterostructured microrods at the tip, end section and entirety (a-c), TEM images for the core-shell heterostructured microrods (d-i).

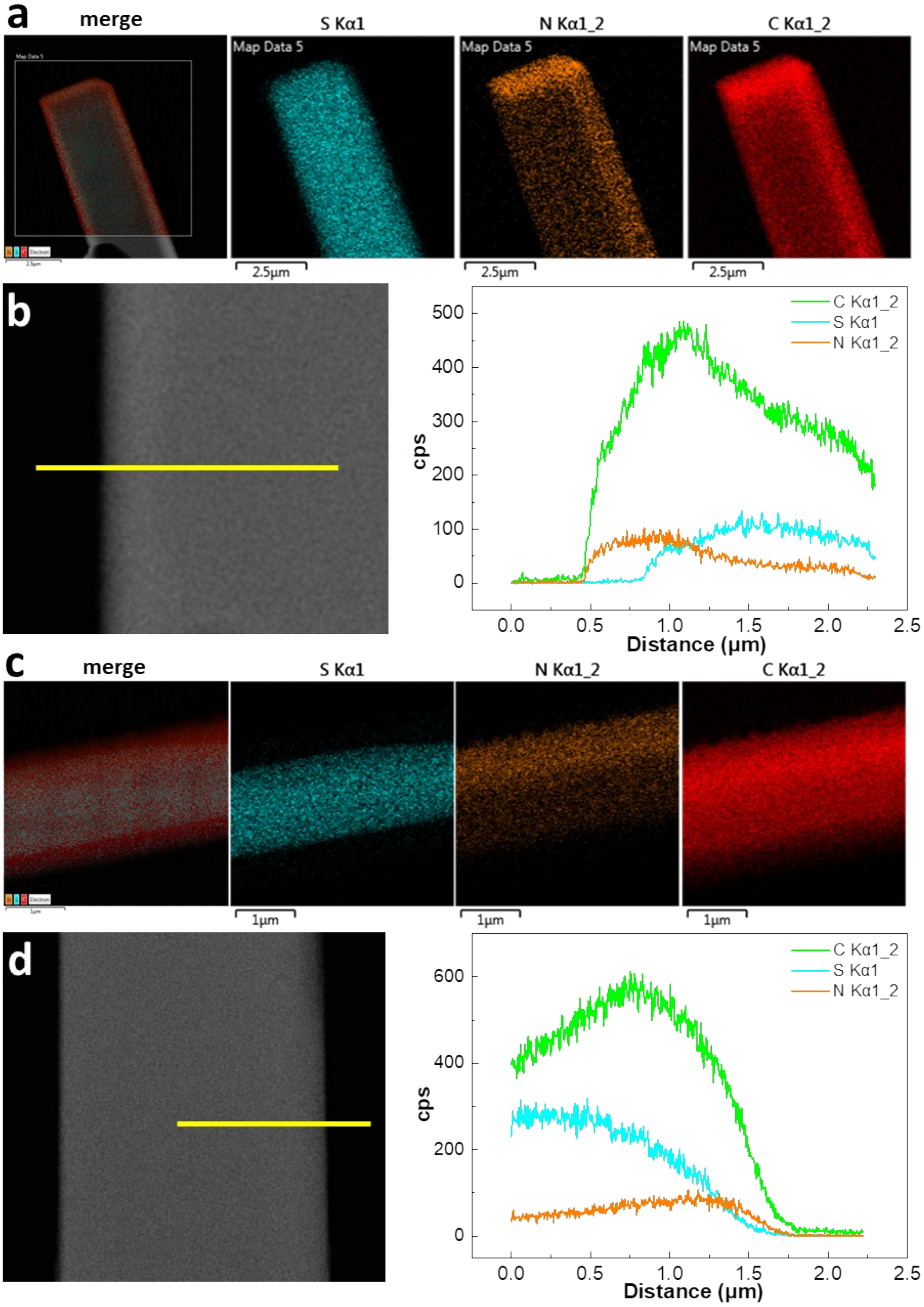

Figure S5. TEM EDS elemental mapping and EDS spectra of elemental line scan of S-TCNB@N-TCNB (a-b), TEM EDS elemental mapping and EDS spectra of elemental line scan of S-TCNB@N-TCNB@C-TCNB (c-d).

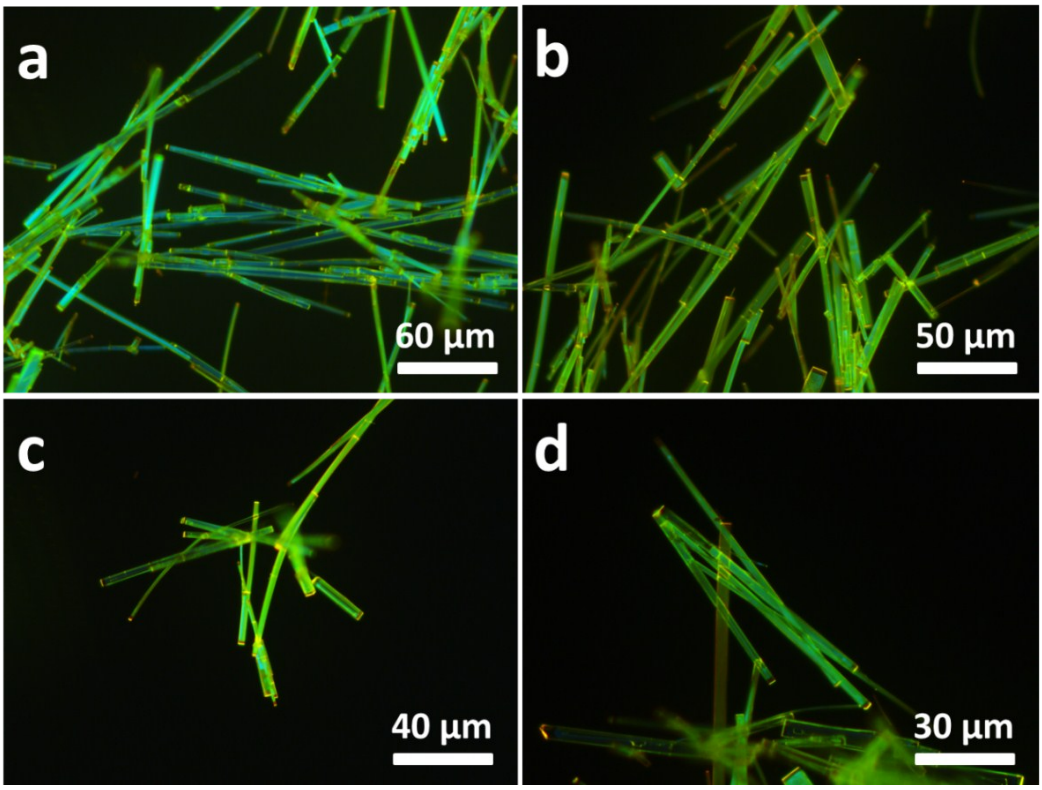

Figure S6. Fluorescent microscopy images for S-TCNB@N-TCNB single-layer core-shell microrods viewed from low to high magnification (a-d).

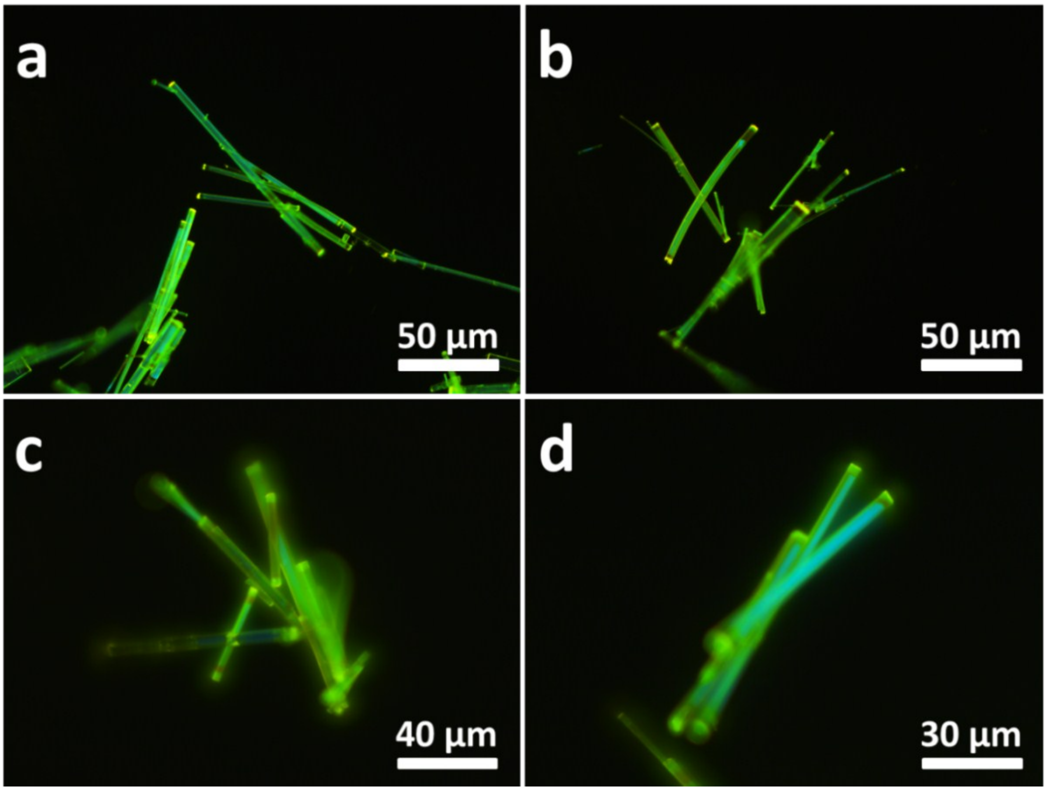

Figure S7. Fluorescent microscopy images for S-TCNB@N-TCNB@C-TCNB two-layer core- shell microrods viewed from low to high magnification (a-d).

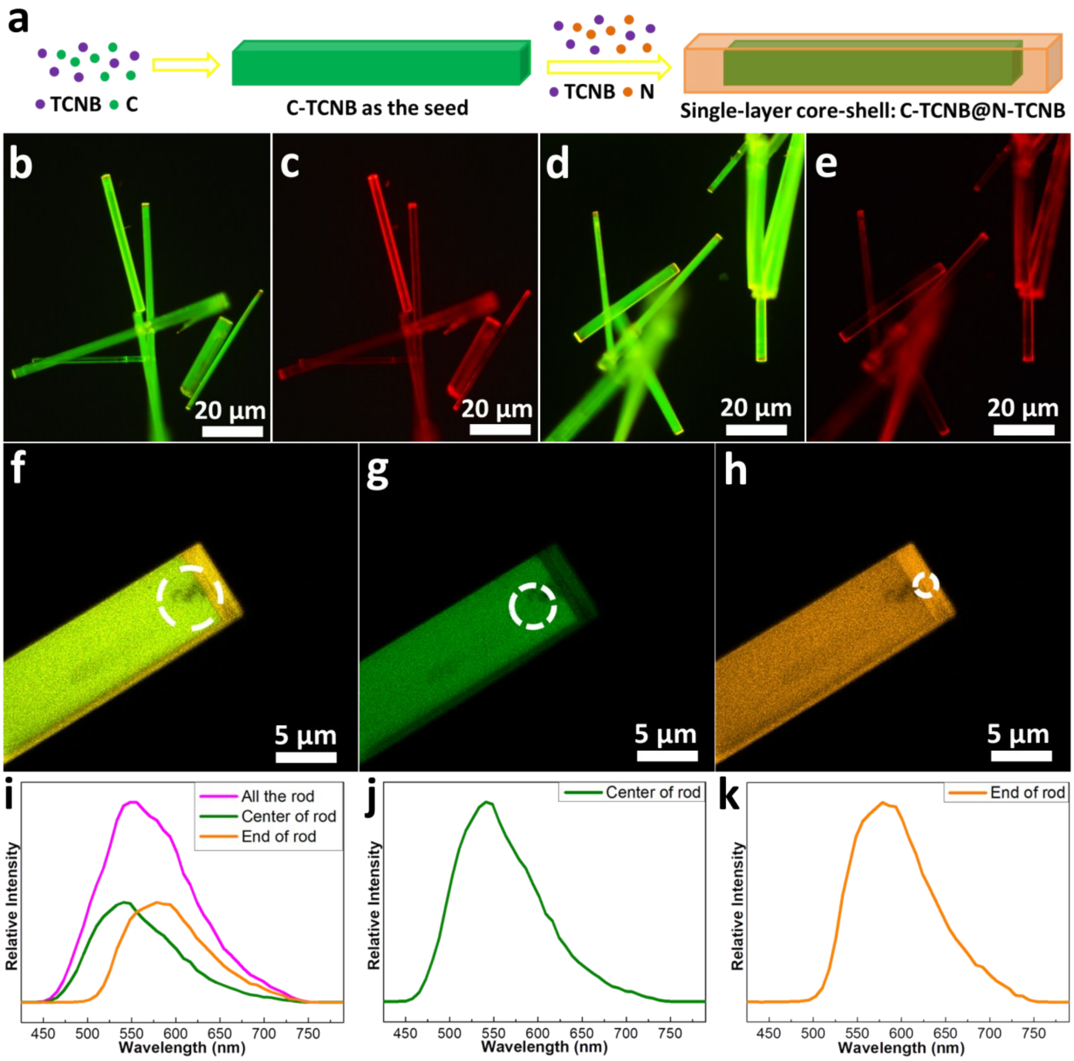

Figure S8. Schematic illustration of the synthetic procedure of C-TCNB@N-TCNB single-layer core-shell microrods by using a stepwise seeded growth method (a). Fluorescence microscopy images of the corresponding rods excited by UV and green light, respectively (b-e). LCFM photographs collected from the green (g), orange (h) light wavelength range and their overlay (f) upon the excitation with blue light (λ_{ex} = 405 nm) with micro-area PL spectra recorded from the selected areas that are marked in white circles on the core-shell rod (f-k).

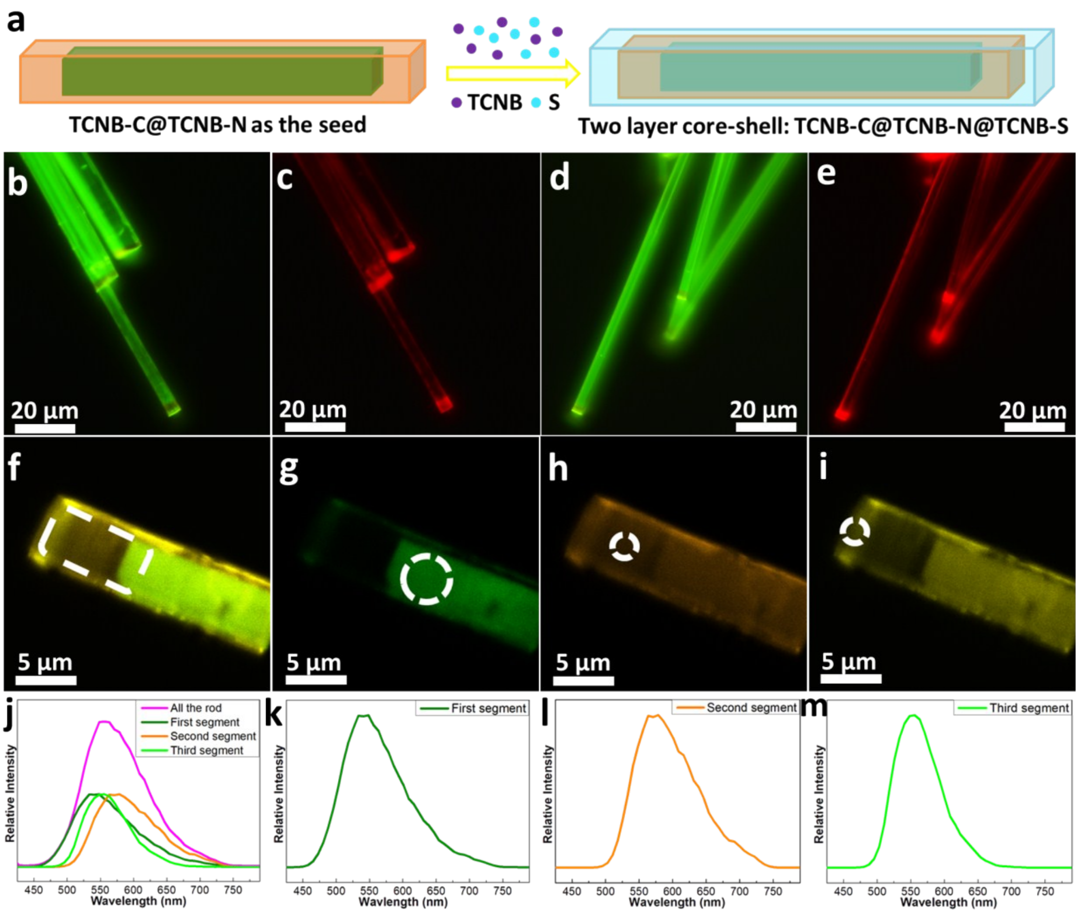

Figure S9. Schematic illustration of the synthetic procedure of C-TCNB@N-TCNB@S-TCNB two-layer core-shell microrods by using a stepwise seeded growth method (a). Fluorescence microscopy images of the corresponding rods excited by UV and green light, respectively (b-e). LCFM photographs collected from the green (g), orange (h), yellow (i) light wavelength range and their overlay (f) upon the excitation with blue light (λ_{ex} = 405 nm) with micro-area PL spectra recorded from the selected areas that are marked in white circles on the core-shell rod (f-m).

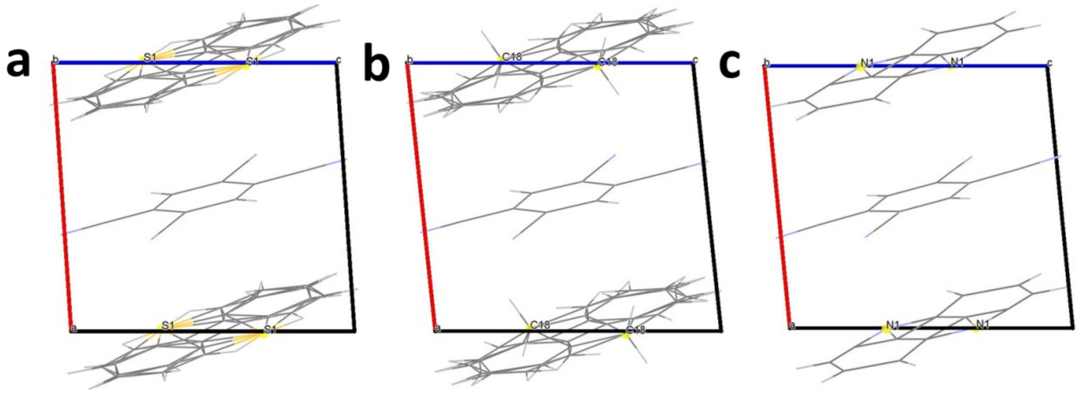

Figure S10. Crystal unit cells of CT complexes S-TCNB (a), C-TCNB (b) and N-TCNB (c) with packing view along the default b axis.

Table S1. Summary of crystallographic data of organic CT complexes S-TCNB, C-TCNB and N-TCNB grown in acetonitrile with ethanol as an induced solvent.

	S-TCNB	C-TCNB	N-TCNB
Empirical formula	$C_{22}H_{10}N_4S$	$C_{23}H_{12}N_4$	$C_{22}H_{11}N_5$
Formula weight	362.40	344.37	345.33
Temperature/K	173(2)	173(2)	100.00(10)
Crystal system	triclinic	triclinic	triclinic
Space group	*P*-1	*P*-1	*P*-1
a/Å	7.1602(16)	7.1773(6)	7.009(4)
b/Å	7.8240(17)	7.7832(6)	7.859(4)
c/Å	7.9224(17)	7.9353(6)	7.860(4)
α/°	72.92(2)	73.799(3)	73.65(4)
β/°	86.08(2)	83.803(3)	84.33(4)
γ/°	89.28(2)	88.445(3)	88.87(5)
Volume/Å^3	423.25(17)	423.19(6)	413.4(4)
Z	1	1	1
ρ_{calc}/g cm^{-3}	1.422	1.351	1.375
μ/mm^{-1}	0.205	0.083	0.689
F(000)	186	178	175
Crystal size/mm^3	0.40×0.30×0.20	0.50×0.45×0.40	0.13×0.12×0.11
2θ range for data collection/°	2.723 to 26.358	2.688 to 26.368	11.736 to 148.842
Index ranges	$-8 \le h \le 8$, $-9 \le k \le 9$, $-9 \le l \le 9$.	$-8 \le h \le 8$, $-9 \le k \le 9$, $-9 \le l \le 9$.	$-6 \le h \le 8$, $-9 \le k \le 9$, $-9 \le l \le 9$.
Reflections collected	6719	5824	2679
Independent reflections	1702 [R(int) = 0.0368]	1723 [R(int) = 0.0281]	1587 [R(int) = 0.0567]
Data/restraints/parameters	1702/0/157	1723/0/157	1587/48/127
Goodness-of-fit on F^2	1.159	0.611	2.595
Final R indexes [I ≥ 2σ(I)]	R1 = 0.0867, wR2 = 0.2777	R1 = 0.0415, wR2 = 0.1008	R1 = 0.0519, wR2 = 0.1221
Final R indexes [all data]	R1 = 0.0910, wR2 = 0.2837	R1 = 0.0466, wR2 = 0.1112	R1 = 0.0732, wR2 = 0.1659
Largest diff. peak/hole/e Å^{-3}	0.918 and -0.460	0.170 and -0.273	0.610 and -0.540

References

[1] Y. Q. Sun, Y. L. Lei, X. H. Sun, S. T. Lee, L. S. Liao, *Chem. Mater.* **2015**, *27*, 1157–1163.

[2] Y. L. Lei, Y. Jin, D. Y. Zhou, W. Gu, X. B. Shi, L. S. Liao, S. T. Lee, *Adv. Mater.* **2012**, *24*, 5345–5351.

[3] A. Arrais, E. Boccaleri, G. Croce, M. Milanesio, R. Orlandoa, E. Diana, *CrystEngComm*. **2003**, *5*, 388–394.